World Meteorological Organization
Organisation météorologique mondiale

Secrétariat
7 bis, avenue de la Paix – Case postale 2300 – CH 1211 Genève 2 – Suisse
Tél.: +41 (0) 22 730 81 11 – Fax: +41 (0) 22 730 81 81
wmo@wmo.int – www.wmo.int

Weather • Climate • Water
Temps • Climat • Eau

MeteoSwiss Payerne CIMO Testbed 2014-2015 report

Terms of Reference for CIMO Testbeds and Lead Centres are available under:
ttp://www.wmo.int/pages/prog/www/IMOP/Testbeds-and-LC.html

Name of Testbed / Lead Centre	**MeteoSwiss Payerne Testbed**
Location of Testbed / Lead Centre	**Payerne, Switzerland**

Contact Person for the Testbed/Lead Centre	
Courtesy Title	Dr
Family name	**Ruffieux**
First name	**Dominique**
Full Postal Address	**MeteoSwiss, Ch de l'Observatoire, 1530 Payerne, Switzerland**
Country	**Switzerland**
Tel. number(s)	**+41 58 460 92 98**
Fax number(s)	**+41 58 460 90 04**
Email(s)	**Dominique.ruffieux@meteoswiss.ch**
Has contact person changed in last 2 years?	Yes / No ? NO
If yes, who was the previous contact person?	

Report on Activities

1. Radiosounding (Rolf Philipona)

1.1 Controlled weather balloon ascents and descents

In situ upper-air measurements are often made with instruments attached to weather balloons launched at the surface and lifted into the stratosphere. Present day balloon-borne sensors allow near-continuous measurements from the Earth's surface to about 35 km (3-5 hPa), where the balloons burst and their instrument payloads descend with parachutes. It has been demonstrated that ascending weather balloons can perturb the air measured by very sensitive humidity and temperature sensors trailing behind them, particularly in the upper troposphere and lower stratosphere (UTLS). The use of controlled balloon descent for such measurements has therefore been investigated and is described here. A new double balloon technique was investigated that uses a carrier balloon to lift the payload and a parachute balloon to control the descent of instruments after the carrier balloon is released at pre-set altitude. This technique has recently been deployed to measure radiation and temperature profiles through the atmosphere. The main reasons for controlled ballooning are: to prevent pendulum motions during ascent, to measure clean, unperturbed air during descent at speeds similar to ascent, and to obtain two vertical profiles at slightly different locations and times with a single balloon launch.

The double balloon technique uses a carrier balloon to lift the payload and a second smaller balloon that acts like a parachute once the carrier balloon is released. Each balloon is fixed to a vertex of a triangular frame of lightweight aluminium that connects them to the payload below (Figure 1). The triangle is equipped with a release mechanism to cut the 20 m string of the carrier balloon at a pre-set altitude. An emergency parachute is fixed between the triangle and the parachute balloon in case the smaller balloon bursts. The large carrier balloon is inflated with enough hydrogen to lift the payload at 5 m/s during ascent while the smaller parachute balloon is inflated with enough helium to maintain a descent rate of ~ 5 m/s once the carrier balloon is released.

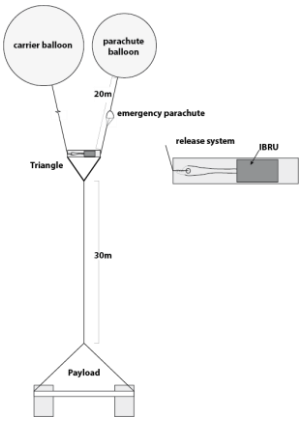

Figure 1 Double balloon sounding configuration with carrier and parachute balloon connected to the payload via the triangle that includes the IBRU release mechanism.

During ascent the two balloons have a tendency to separate, with the larger balloon leading. The triangle between the two balloons acts as a fix point stabilizing the payload. Comparisons have clearly shown that the pendulum motion usually observed on single balloon flights is strongly reduced with the double balloon technique. Figure 2 (left panel) shows the horizontal travel of the payload over the first 2000 m of ascent during two simultaneous radiosonde flights, one using the traditional single balloon configuration (blue) and the other utilizing the double balloon (red) method. The two radiosondes travel in the same general direction but the single balloon payload moves in circles of up to 10 m radius due to pendulum motion while the double balloon payload

does not. The reduced pendulum motion of the double balloon method is very important for radiation measurements where instruments need to remain as horizontal as possible during flight.

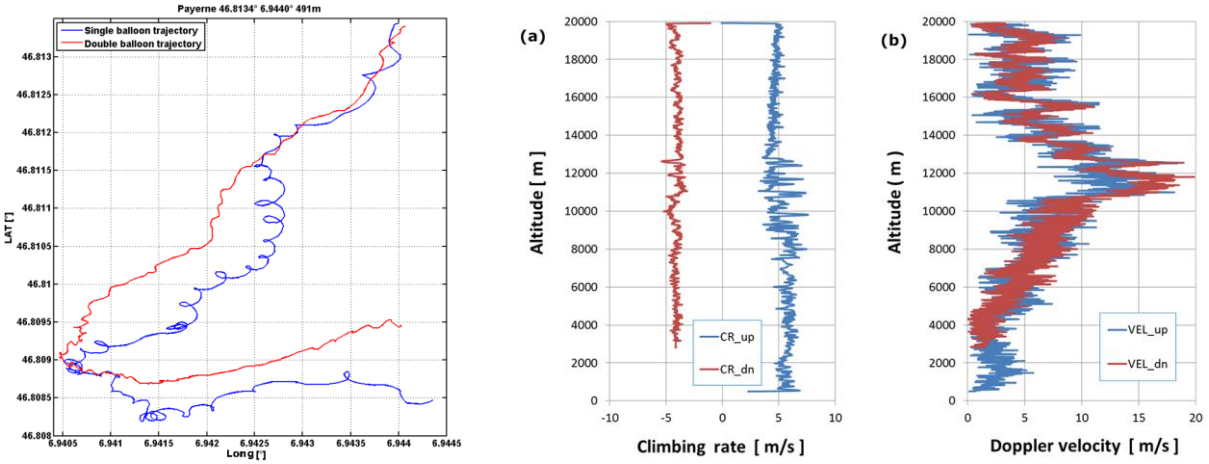

Figure 2 Left panel: horizontal trajectories of two radiosonde flights launched simultaneously at Payerne, Switzerland, on 12 May 2011. The two curves show the GPS latitude and longitude coordinates over the first 2000 m of ascent for the standard single balloon configuration (blue) and the double balloon configuration (red). Right panels: double balloon flight to 20 km and back. Graph a) shows the ascent and descent rates as functions of altitude. Graph b) shows the Doppler velocity with considerable less noise during the descent than during the ascent, which demonstrates that for the double ballooning method the descent is more quiescent than the ascent.

The double balloon method also improves the stability of descent rates compared to ascent rates. Two SRS-C34 radiosondes were flown together using a 1200 g carrier balloon and an 800 g parachute balloon. The IBRU was set to release the carrier balloon at 20 km. Figure 2 (central panel, a) shows the ascent and descent rates of the payloads as a function of altitude. The ascent rate averaged 5 ± 0.8 m/s (1σ), whereas the mean descent rate of 4 ± 0.3 m/s was slightly slower but more consistent during the entire descent. Figure 2 (right panel, b) shows the Doppler velocity, which is the instantaneous movement of the radiosonde measured by the GPS. During the descent the noise of the Doppler velocity is considerably lower, which demonstrates that the descent is more quiescent than the ascent despite double ballooning.

Some radiosonde sensors do not perform as well during descent because their orientations are optimized for best performance during ascent. There are three main factors for sensors that differ between ascent and descent: the direction and strength of ventilation flow past the sensor, the vertical structure of the parameter being measured and the vertical gradient of environmental parameters such as temperature. In contrast to most other radiosondes the thermocouple temperature sensor of the Meteolabor SRS-C34 radiosonde is not mounted in a sensor boom, but is fixed to thin wires that extend at a 45° angle upward and is at least 100 mm away from the radiosonde (Figure 3). Thus, the airflow around the radiosonde is not guided over the temperature sensor during the descent. According to the last WMO intercomparison, the uncertainty of SRS-C34 daytime temperature measurements is less than 0.2°C in the troposphere and about 0.4°C in the upper stratosphere (Nash et al., 2011). Figure 4 a) and b) show ascent and descent temperature profiles of two SRS-C34 radiosondes flown about 2 m apart on a bamboo boom during the 20 km flight. The two panels show that ascent and descent profiles are very similar and that small temperature differences between them at about 5000, 13000 and 15500 m are measured by both radiosondes. The temperature differences measured between sonde 1 and sonde 2 are shown in Figure 4 c) for the ascent and the descent. The temperature differences (descent minus ascent) presented in Figure 4 d) shows that both sondes measured similar differences at all altitudes for the 1000 m resolution (thick lines) as well as for the 100 m resolution (thin lines).

Figure 3 Meteolabor SRS-C34 radiosonde with original thermocouple temperature sensor fixed to thin wires that extend at a 45° angle upward (above right) and an additional thermocouple at a 45° angle downward (below right).

To check if the temperature sensors mounted above the radiosonde measure correctly during ascent and descent, the two radiosondes were equipped with additional temperature sensors fixed to thin wires extending downward from the bottom of the radiosonde at a 45° angle and 100 mm away from the box. Temperature measurements by the bottom sensors (Figure 4, right panels) are very similar to those by the top sensors (Figure 4, left panels). The two figures demonstrate that the 100 m resolution ascent-descent measurement disparities at particular locations (5000, 13000 and 15500 m) are real differences in the atmosphere. With the ascent starting around 10:00 local time on a more or less cloud free day, the measurements show temperature profiles during ascent and descent that are within 0.4 °C (1000 m resolution), except around 13000 m, where the atmosphere was apparently slightly colder during the descent. On the other hand slightly warmer temperatures were measured in the lower troposphere during descent, which is reasonable given the normal daytime temperature increase after 10:00.

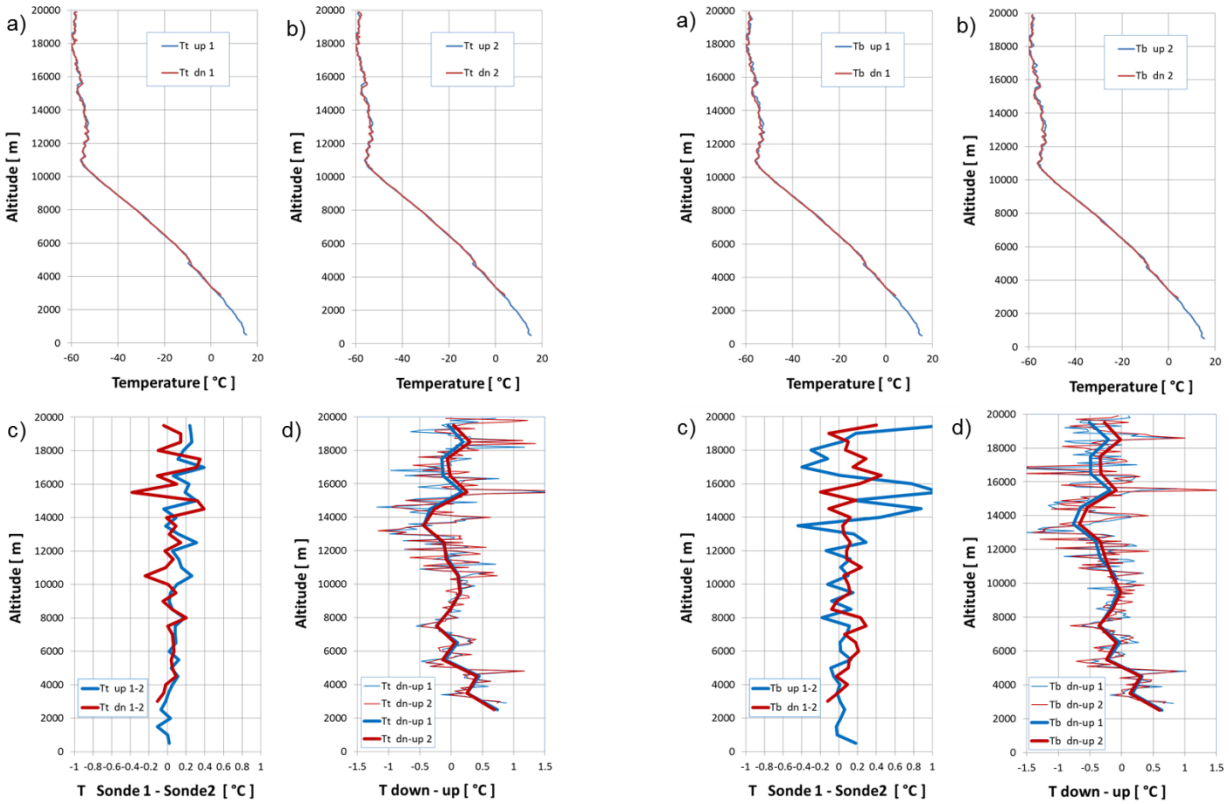

Figure 4 Left panels: temperature measurements by two SRS-C34 radiosondes during ascent to 20 km and controlled descent using standard temperature sensors (Tt) mounted to the top of the radiosondes. Shown are (a) ascent and descent temperature profiles measured by sonde 1, (b) same as (a) but measured by sonde 2, (c) temperature differences between the two sondes and (d) descent-ascent temperature differences for each of the two sondes at vertical resolutions of 100 m (thin curves) and 1000 m (thick curves). Right panels: temperature measurements by two SRS-C34 radiosondes during ascent to 20 km and controlled descent using additional temperature sensors (Tb) mounted to the bottom of the radiosondes. Shown are (a) ascent and descent temperature profiles measured by sonde 1, (b) same as (a) but measured by sonde 2, (c) temperature differences between the two sondes and (d) descent-ascent temperature differences for each of the two sondes at vertical resolutions of 100 m (thin curves) and 1000 m (thick curves).

Reference:
Kräuchi, A., Philipona, R., Romanens, G., Hurst, D. F., Hall, E. G., and Jordan, A. F.: Controlled weather balloon ascents and descents for atmospheric research and climate monitoring, Atmos. Meas. Tech. Discuss., 8, 12559-12588, doi:10.5194/amtd-8-12559-2015, 2015.

1.2 Return glider radiosonde for in-situ upper-air research measurements

Upper-air balloon soundings for weather predictions have been made since the beginning of the 20th century. New radiosonde instruments for in-situ humidity-, radiation- and gas profile measurements in the troposphere and the lower stratosphere, were introduced in recent years for atmospheric research and climate monitoring. Such instruments are often expensive and aimed at being reused on many flights. However, recovering instruments that freely descent with parachutes is time-consuming and sometimes difficult and even dangerous. A new Return Glider Radiosonde (RGR), which enables flying and retrieving valuable in-situ upper-air instruments, was therefore build. The RGR is lifted with weather balloons similar to traditional radiosondes to a pre-set altitude, at which time a release mechanism cuts the tether string, and a built in autopilot flies the glider autonomously back to the launch site or a desired preprogramed location. Once the RGR reaches the landing coordinates it circles down and releases a parachute 100 m above ground for landing. The motivation for this project was to measure radiation profiles throughout the atmosphere with the same instrument multiple times. Several successive flights measuring radiation profiles demonstrated the reliability and the operational readiness of the RGR, allowing new ways for atmospheric in-situ research- and monitoring measurements with different built-in sensors and instruments to be utilized.

The return glider radiosonde is based on the experience made with the double balloon technique, but uses a new technology to fly back the payload after measurements are completed. The RGR consists of a flying wing with a built-in radiosonde, a release mechanism, an autopilot and a parachute for autonomous landing. It was conceived for atmospheric radiation profile measurements. Short- and longwave radiation sensors, which are controlled by the radiosonde, are therefore integrated in the wings of the glider. To stay within the payload limitations of a balloon born sounding, it was important to keep the weight of the fully equipped aircraft as low as possible. Therefore the flying wing was designed without a propulsion system to reduce the weight.

The flying wing has a wingspan of 1.4 m and is made out of the special foam EPP, which is covered with a 100 m thin laminate film to protect the EPP foam (Figure 5). The aircraft is controlled by two control surfaces, called elevons. All electronics except the servos that control the elevons are stored inside the payload area in the middle section of the flying wing, which is made out of two Styrofoam boxes that allow maximum storage space for the radiosonde, batteries, the release mechanism and the navigation control devices. The boxes are glued on top of each other and designed for radiosonde application to withstand extreme cold temperatures even under high airflow when flying back.

The scientific instruments, in this case the short and longwave radiation sensors, are integrated into the left and right wing. The instrument body has the same height as the thickness of the wing, therefore only the instrument domes protrude and all cables and connectors are inside the wing, which is connected to the radiosonde in the payload section. Temperature and humidity are measured at the back of the glider with the thermocouple temperature sensor slightly extending upward to prevent temperature perturbations of the glider.

In the front of the middle section a parachute is embedded into a Styrofoam half sphere. The parachute is used for the landing and also serves as emergency recovery system if the autopilot detects any malfunction. The total weight of a fully equipped return glider radiosonde with batteries and radiation instruments is under 2 kg and is within the limits of standard balloon born payloads.

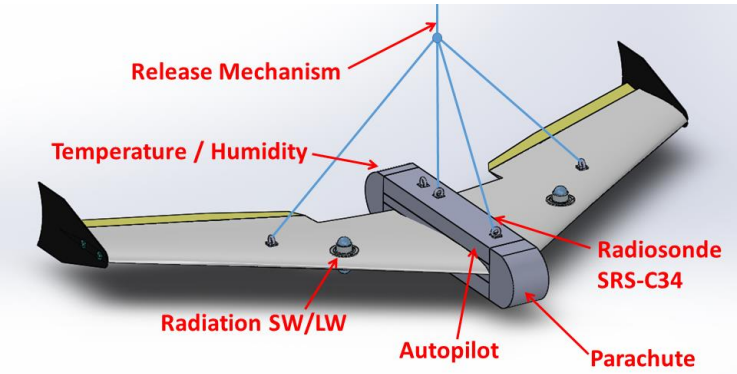

Figure 5 A three dimensional view of the return glider radiosonde (RGR), including the middle payload section where the electronic is stored, and the two short and longwave radiation instruments mounted in the wings.

We first conducted night time flights in Switzerland to test all electronics and software algorithms. While working with the Federal Office of Civil Aviation (FOCA) we were also in contact with FINAVIA in Finland, who allowed us to do test flights with the RGR at the arctic research center Sodankylä, of the Finnish Meteorological Institute (FMI). The permission included day and night flights up to 30'000 m. The Sodankylä facility is an aerological sounding station in operation since 1949 and has recently become a GRUAN station.

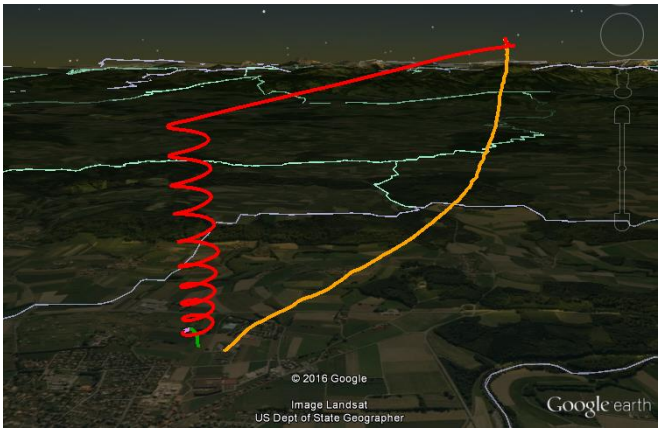

Figure 6 3D view of the first flight path performed from the aerological station in Payerne Switzerland. Orange: ascending path with the balloon; red: glider flight path back to the landing coordinates; green: parachute landing.

To stay within the limits set by FOCA a calm night in terms of wind speed was required for a first test flight in Payerne. The RGR was set to release the balloon at 2200 m above sea level and then return to the grassland next to the aerological station. After an 8 minute ascend the RGR released the balloon and after a short flight of less than one minute the landing coordinates were reached 1 km above ground, where the RGR started to circle down. Only 15 minutes after the balloon start the RGR landed safely with the parachute on the grassland (Figure 6).

With the successful flight in Switzerland the goals for the campaign in Sodankylä, during the first two weeks of July, were to test the RGR at high altitudes, and to learn how it handles different wind conditions and from how far it can fly back to the release point. Additionally, the overall performance and reliability of the autopilot and the gliders structure were analyzed. The radiation profiles measured during the flights, under very different atmospheric conditions, were both very successful and interesting.

During several test flights from 24 km altitude the RGR proved to reliably control itself, and to maintain its flight even if very strong winds push the glider backward. Analyses showed that the RGR maintains a forward flight path with head winds of up to 20 m/s. The overall glide ratio during flights from various altitudes is 5.5:1, which from 24 km altitude results in a flight distance of roughly 130 km. This maximum flight distance can only be achieved during calm wind conditions and is reduced once the RGR passes different wind speed layers. Emergency landing points along

the flight path allow flights even during strong winds since the autopilot is capable of detecting unfavorable wind conditions and reacting accordingly.

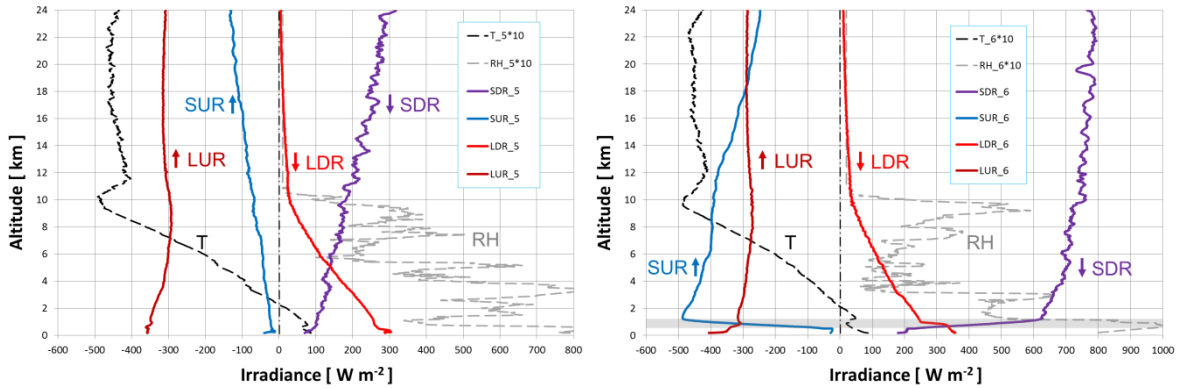

Figure 7 Temperature, relative humidity and radiation profile measurements with the RGR to an altitude of 24 km. Flight #5 (left) started in the early morning and flight #6 (right) six hours later. The morning flight was cloud free, whereas at noon a thin cloud layer between 500 and 1200 m shows the strong influence of clouds on shortwave and also longwave radiation. Downward SDR and LDR fluxes are positive and upward SUR and LUR fluxes are negative. Temperature and relative humidity signals are multiplied by a factor of ten.

The motivation to build the RGR was to routinely measure radiation profiles through the atmosphere for climate change investigations. Figure 7 shows radiation profiles measured to 24 km during two successive flights within 6 hours at Sodankylä. The first flight was in the early morning showing small downward and upward solar irradiance. During the second flight around noon a thin cloud layer between 500 and 1200 m led to a temperature inversion, and shows a large increase of shortwave down- and upward radiation through the cloud and also the influence on the longwave radiation profiles. Comparing radiation profiles that were taken under different weather conditions allows studying effects of air temperature, water vapor, clouds, ozone and other greenhouse gases on solar and thermal radiation and the radiation budget in the atmosphere.

Using the concept of traditional radiosondes on the RGR allows connecting different upper-air research instruments, and transmitting measured physical values and all important information from the autopilot continuously to the ground station. Moreover, the system is fully autonomous relying only on preset values without receiving information from the ground. The RGR has successfully been used to measure radiation profiles through the atmosphere, but many different in-situ research- or climate monitoring measurements can be made that rely on multiple flights with the same instruments, or use specific sensors that need post processing analyses after the flight.

Reference:
Kräuchi, A. and Philipona, R.: Return glider radiosonde for in-situ upper-air research measurements, Atmos. Meas. Tech. Discuss., doi:10.5194/amt-2016-35, in review, 2016.
http://www.atmos-meas-tech-discuss.net/amt-2016-35/

2. Ground-based remote sensing (Alexander Haefele)

2.1 Raman lidar

The Raman lidar deployed at the Payerne site since 2008 is designed to measure humidity, temperature and aerosol profiles for operational meteorology and for long term observations of high quality. A big effort has been made to make the system fully automatic and to achieve a data availability of more than 50% on the basis of several years. This very high availability for a Raman lidar is operationally obtained ever since.

During these last two years, the main activities focused on several topics.

- **Calibration**

In order to improve calibration of the water vapor measurements a system based on a reference lamp has been installed. Calibration data are acquired once per night and processed automatically.

- **Upgrade of the Raman lidar with a new temperature module (PRR)**

In close collaboration with the EPFL, a new module using fast acquisition was installed on the system. It is now possible to estimate temperature profiles every 30 minutes, weather permitting (Figure 8). This new and essential information is now going through a validation process.

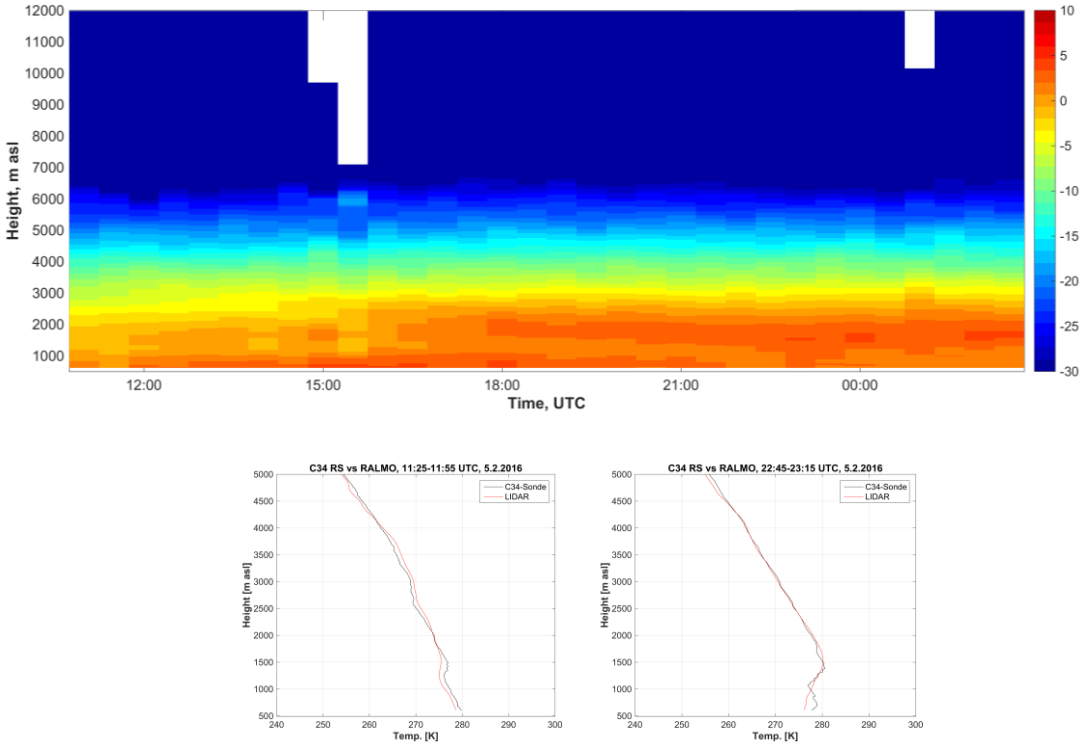

Figure 8 Raman lidar temperature profiles, Payerne, 5 February, 2016. Upper panel: time series (color scale in degrees C); lower panels: single lidar profiles (red) compared to radiosounding temperature profiles (black).

– **Development of a 1D-var retrieval for elastic backscatter and water vapor.**

During the 2014/2015 sabbatical of Prof. Bob Sicca (University of Western Ontario, Canada) at MeteoSwiss Payerne, an Optimal Estimation Method (OEM) was developed for the retrieval of water vapor mixing ratio, aerosol optical depth profile, Ångstrom exponent, lidar constants, detector dead times and measurement backgrounds from multichannel vibrational Raman scatter lidar data. The OEM retrieval provides, in addition to the random uncertainties due to measurement noise, the systematic uncertainties due to the lidar's overlap function and lidar calibration factor, the assumed air density and the Rayleigh-scatter cross sections. The OEM also gives the vertical resolution of the retrieval as a function of height, as well as the height to which the contribution of the a priori is small. The retrieval is demonstrated to give excellent results as compared to the traditional lidar retrieval method as well as with coincident radiosoundings, using measurements in both clear and cloudy conditions, during both the daytime and nighttime.

Related publications:

Sicca, R.J., and A. Haefele, 2015: Retrieval of Temperature From a Multiple Channel Raman-Scatter Lidar Using an Optimal Estimation Method. Applied Optics, Vol.54, No.8, 1872-1889. http://dx.doi.org/10.1364/AO.54.001872.

Sica, R.J., and A. Haefele, 2016: Retrieval of water vapor mixing ratio from a multiple channel Raman-scatter lidar using an optimal estimation method, Appl. Opt. 55, 763-777.

– **Generation of O-B statistics using Raman lidar and COSMO humidity profiles.**

Observation minus background (O-B) statistics have been derived for humidity from Raman lidar and COSMO-2 data. The (Figure 9) shows the bias and standard deviation of O-B for different lead times for the 00h UTC run. While the bias stays relatively constant over a 3h forecasting period, the standard deviation increases from 20 to 30% over 3h at 4000 m. This error growth increases with altitude. Note, that at 00h UTC the radiosonde is assimilated into the model, hence the bias and standard deviation of the model analysis is relatively small and comparable to the radiosonde.

It could be shown that for the 21h run the bias and standard deviation are significantly bigger and no error growth can be observed, which leads to the conclusion that no update of the humidity field takes in this assimilation cycle. This is due to the lack of continuous humidity observations.

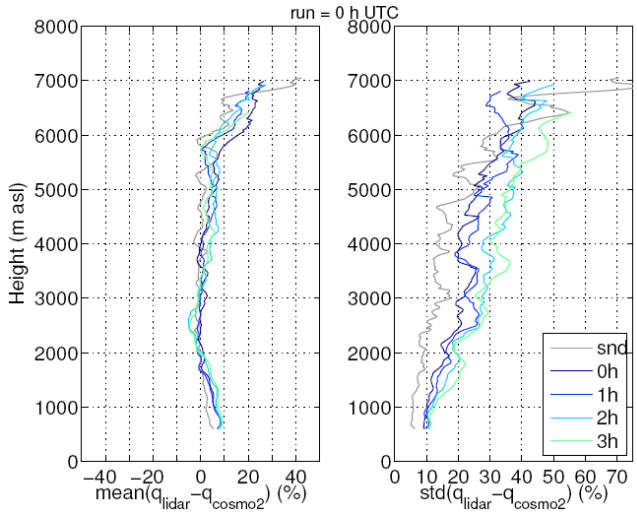

Figure 9 Mean (left panel) and standard deviation (right panel) of the differences between lidar, radiosonde (grey lines), and various lead times of COSMO2 for the 00h UTC run.

– **Contribution to NDACC, GRUAN, NWP**

The data from various systems operated at Payerne and including the Raman lidar are operationally transmitted to NDACC and WMO-GRUAN as well as for NWP models for assimilation (radiosoundings, radar wind profilers) and validation (Raman lidar, microwave radiometer).

2.2 Automatic elastic lidar ceilometer

In the last years it has been realized that the new generation of ceilometers can not only provide cloud base height but also valuable information of the vertical distribution of aerosols. After the eruption of the Eyjafjellajökull volcano in 2010 the ashes have been detected at several sites with advanced ceilometers. Given the relatively low costs and the consequently high density of these instruments, ceilometers have a big potential in the field of aerosol monitoring in the boundary layer and the free troposphere. Calibration of ceilometers is an important step towards data harmonization and quantitative interpretation of the data. In the frame of the EUMETNET program E-PROFILE and the COST action TOPROF calibration procedures are being developed and validated. The Payerne site is taking a leading role in several domains:

- **MeteoSwiss** is actively participating to two important international programmes: the Payerne station has the leadership of the EUMETNET E-Profile Programme as well as the Vice-Chairmanship of the COST Action TOPROF "Towards operational ground based profiling with ceilometers, doppler lidars and microwave radiometers for improving weather forecasts".
- **An automatic correction of the overlap function of the CHM15K ceilometer** was developed and applied to several ceilometer systems. Imperfections in a lidar's overlap function lead to artefacts in the background, range and overlap corrected lidar signals. These artefacts can erroneously be interpreted as an aerosol gradient or, in extreme cases, as a cloud base leading to false cloud detection. A correct specification of the overlap function is hence crucial to use automatic elastic lidars (ceilometers) for the detection of the planetary boundary layer or low clouds.

Publication:

Hervo M, Y Poltera, and A. Haefele, 2016: An empirical method to correct for temperature dependent variations in the overlap function of CHM15k ceilometers. Atmos. Meas. Tech. Discuss., doi:10.5194/amt-2016-30.

- **Operational estimation of the planetary boundary layer**

The planetary boundary layer height (PBL height) is an important parameter for air quality and the

dispersion of pollutants in the atmosphere. Four different algorithms have been applied to remotely sensed temperature, humidity, wind and aerosol profiles for a continuous monitoring of the boundary layer. The automatic detection of the PBL using ground-based remote sensing systems is still in progress. A publication on retrieval of the PBL using pathfinder methods is in preparation.

2.3 Microwave radiometer profilers

Two microwave radiometers are operationally used in Payerne. The SOMORA ozone profiler is running at 142GHz while the commercially available HATPRO (20-50GHz) provides temperature and water vapor profiles in real-time. Homogenization of the ozone time series (in operation since 2000) is currently under way while. The temperature profiles show still some unexplained biases for which an automatic correction scheme is currently implemented. Finally, HATPRO information is operationally used for the planetary boundary layer detection over Payerne.

2.4 Radar wind profilers

The radar wind profiler of Payerne is one segment of the nuclear power plant meteorological surveillance system of Switzerland. Improvement of the system includes some hardware and software upgrades improving the temporal resolution and reducing the external contaminations (i.e. using Gabor algorithm).
The calculation of uncertainties related to radar wind profilers was analysed by validating profiles from the system at Payerne with 3 years of co-located radiosoundings.

Publication:
Haefele A., and D. Ruffieux, 2015: Validation of the 1290 MHz wind profiler at Payerne, Switzerland, using radiosonde GPS wind measurements. *Meteorol. Appl.* (2015), DOI: 10.1002/met.1507.

3. Performance evaluation of radiation sensors for the solar energy sector (Laurent Vuilleumier)

3.1 Introduction

In the previous reports, a contribution for evaluating the performance of radiometers designed for the solar energy sector was described. This was an effort to better understand the performance of these instrument within an emerging “regulatory” framework (e.g., standard operating procedures, certification, traceability, etc.) for such monitoring**.**

This activity included the organization by MeteoSwiss of an inter-comparison of radiometers measuring Direct Normal solar Irradiance (DNI) from 15/06/2012 to 15/09/2013. The goal was comparing target instruments to high accuracy radiation monitoring instruments (references) from the Baseline Surface Radiation Network (BSRN) Payerne site. The analysis is now achieved, and final results can be provided.

The target instruments are Rotating Shadowband Irradiometers (RSI) and SPN1 Sunshine Pyranometers. The RSI and SPN1 instruments allow separately inferring the diffuse and direct component of solar radiation without sun trackers; they are robust, compact, lightweight with low power consumption, and can be deployed in networks for continuous field operation with limited maintenance. The analysis was applied both to the whole dataset and data subsets reflecting particular conditions (high or low solar elevation, high or low DNI variability) to allow a better understanding of how the instruments performances depend on such conditions.

A refereed journal paper described the accuracy of the reference instruments (Vuilleumier et al., 2014), two other referred papers described various aspects of the inter-comparison (Badosa et al., 2014; Vignola et al., 2016) and a report is in preparation for describing the performance evaluation of the radiometers designed for the solar energy sector. The conclusions of this report are given below.

3.2 Evaluated instrument performances

This study focused on the error of the tested instruments with respect to well characterized references and uses statistical indicators such as median, MAE, RMSE, inter-quartile range, and an extended range of the error distributions. The analysis was also applied on data subsets reflecting particular conditions (high or low solar elevation, high or low DNI variability) for better understanding of the dependences of the instrument performances on such conditions. This helps understanding how the uncertainty could change for different locations and atmospheric conditions. Caution must however be exercised in generalizing the results of this study, because at some locations the conditions are too far from those experienced at Payerne. For instance, the integrated water vapor column is almost always significant over Payerne, so it may not be possible to generalize the results of this study to locations with quite dry atmosphere such as arid regions or high elevation sites. The same comment stands for the solar elevation which is limited to 67° at Payerne.

The overall performance of the tested instruments for measuring global horizontal irradiance (GHI) is not as good as this of the reference instruments described by (Vuilleumier et al., 2014). But it is nonetheless satisfactory as none of the instruments exhibit error distributions significantly exceeding about ±30 Wm^{-2}, which would be the agreement expected for instruments with an expanded uncertainty of ±25 Wm^{-2} (±10%). For diffuse horizontal irradiance (DfHI), RSIs exhibited errors on the order of ±20 Wm^{-2} (±13%) with some of them being affected by small systematic negative biases on the order of -5 Wm^{-2} (median). SPN1s instruments underestimate DfHI by about -10 Wm^{-2} (median of the error distribution) with a relatively large range of the expanded error distribution between -45 Wm^{-2} and 20 Wm^{-2} (-35% to 13%). For direct normal irradiance (DNI), the extended range of the error distribution for RSI is on the order of ±40 Wm^{-2} (±5-6%) with some instruments presenting no bias while others are affected by median biases up to -15 Wm^{-2}. SPN1 instruments exhibit a relatively large median bias of 40 Wm^{-2}, and an extended range of the error distribution between -45 Wm^{-2} and 125 Wm^{-2} (-6% to 19%).

The GHI and DfHI errors of RSIs were found to be very similar, especially for favorable conditions. They also showed similar dependences on solar elevation. DNI errors significantly smaller in relative value than GHI or DfHI errors were found, suggesting a cancelation of error when inferring DNI from GHI and DfHI. Such an error cancelation process requires the GHI and DfHI errors of RSIs to be correlated, which is also corroborated by their similar solar elevation dependence.

Despite these similarities, the cause of RSI GHI and DfHI errors seem to be different. The GHI error solar elevation dependence seems to be linked to the increase of the GHI signal as solar elevation increases, while another –or an additional– cause is necessary to explain the DfHI solar elevation dependence, most likely spectral effects related to the non-uniform spectral response of the RSI sensor. Unfortunately, even though the dataset used in this analysis is quite comprehensive, this hypothesis could not be demonstrated in a definitive manner. Spectral data were only available for DNI. (Vignola et al., 2016) specifically analyzed the influence of the non-uniform spectral response of the LICOR sensor on the detection of shortwave radiation for DNI using these data. Ideally, if spectral data had been available for DfHI and DNI, such an analysis could have been extended to DfHI.

The RSIs appear to be optimized for providing good estimates of DNI and the related accuracy is very satisfactory; the uncertainty is about twice the uncertainty of a “good quality pyrheliometer” (World Meteorological Organization, 2010) in favorable conditions, even though DNI is not measured directly but inferred. Reducing this uncertainty further would be challenging. It would require a detailed understanding of the DfHI and GHI errors to reduce them in a first step, followed by an optimization of the corrections applied when inferring the DNI itself. For GHI, the RSI have performances that would place them at the limit between “moderate” and “good quality pyranometers” (World Meteorological Organization, 2010).

The SPN1 instruments, contrary to RSI, exhibit errors that tend to be of opposite signs for GHI and DfHI, especially in favorable cases: slightly positive GHI median errors and significantly negative DfHI median errors. When inferring DNI, it results in an addition of errors that is further amplified by the presence of the sine of the solar elevation $\sin(\xi_s)$ in the denominator. In difficult cases, the DfHI errors are smaller, but because the solar elevation is low the error amplification due to $\sin(\xi_s)$ is

stronger. The resulting errors when simply inferring DNI from the difference between GHI and DfHI are large. While the SPN1 performances for measuring GHI are similar to those of RSI, corrections are required to obtain satisfactory performances for DNI.

A correction based on the detailed understanding of the source of the error would be the best option, but such a correction proved difficult to devise until now. (Badosa, et al., 2014) proposed some empirical corrections. Given the homogeneity of the dependence of the DNI error distribution on solar elevation, it could be appropriate to explore a $\sin(\xi_s)$ dependent correction, possibly also depending on the cloud cover. However for these instruments, there is also a strong potential of improvement for DfHI, and thus for DNI, if derived from the difference between GHI and DfHI.

This analysis was performed using 1-minute data. Aggregating the data on longer time steps usually improve the performances of instruments because of a reduction of the random part of the error through averaging. A power spectral density analysis applied on DNI data showed that such improvement mostly occur when aggregating on timescale up to about 1 hour. Aggregating beyond these timescales provides little further gain in performance.

This study analyzed the performances of GHI, DfHI and DNI measurements performed by the instruments under study in standard operating conditions, although they were well maintained during the whole study. For instruments that would be less well maintained (remote operation with little on-site maintenance), the main problem is anticipated to be soiling. (Michalsky, et al., 1988) and (Geuder and Quaschning, 2006) investigated the effect of soiling on RSI, and found that such instruments are less affected by soiling than other types of radiometers. There is no study known to the authors investigating the effect of soiling on SPN1 instruments. This study further explored how the instrument uncertainty depended on the operating conditions, but it remains not fully generalizable. It would be useful to repeat such a study under different climatic conditions, e.g., dryer or more humid environments (arid regions or high elevation sites vs. tropics) to assess the transferability of the results obtained here. It would be especially useful in such studies to also deploy instruments allowing spectral measurements of both DNI and DfHI on a wide wavelength spectrum. Similarly, an instrument able to measure the energy available in the sun aureole would help improving the understanding of geometrical or directional error sources.

References cited :

Badosa, J., J. Wood, P. Blanc, C. N. Long, L. Vuilleumier, D. Demengel, and M. Haeffelin (2014). Solar irradiances measured using SPN1 radiometers: uncertainties and clues for development, , Atmospheric Measurement Techniques, 7, 4267-4283, doi:10.5194/amt-7-4267-2014.

Geuder, N. and Quaschning, V. (2006). Soiling of irradiation sensors and methods for soiling correction. Solar Energy, 80(11), 1402-1409. doi: 10.1016/j.solener.2006.06.001.

Michalsky, J., Perez R., R., Stewart, R., LeBaron, B. A. and Harrison, L. (1988). Design and development of a rotating shadowband radiometer solar radiation/daylight network. Solar Energy, 41(6), 577-581. doi: 10.1016/0038-092X(88)90060-6.

Vignola, F.; Derocher, Z.; Peterson, J.; Vuilleumier, L.; Félix, C.; Gröbner, J., and Kouremeti, N. (2016). Effects of changing spectral radiation distribution on the performance of photodiode pyranometers. Solar Energy, 129, 224-235, doi: 10.1016/j.solener.2016.01.047.

Vuilleumier, L., M. Hauser, C. Félix, F. Vignola, P. Blanc, A. Kazantzidis, and B. Calpini (2014). Accuracy of ground surface broadband shortwave radiation monitoring, J. Geophys. Res. Atmos., 119:D24, 13'838-13'860, doi:10.1002/2014JD022335.

World Meteorological Organization, 2010. Guide to Meteorological Instruments and Methods of Observation, Geneva, Switzerland: WMO-No. 8., World Meteorol. Organ., Geneva, Switzerland.

4. The SwissMetNet network and the CIMO SPICE experiment (Yves-Alain Roulet and Audrey Reverdin)

4.1 SwissMetNet

The renewal and extension of the ground-based meteorological network of MeteoSwiss, SwissMetNet, has been completed by the end of 2015. The final state of the SwissMetNet network (Figure 10) consists of 150 fully equipped ground-based meteorological stations (measuring the main atmospheric parameters) and 120 additional sites for precipitation measurement only (for specific needs on severe weather monitoring and for automation of long series manual measurement).

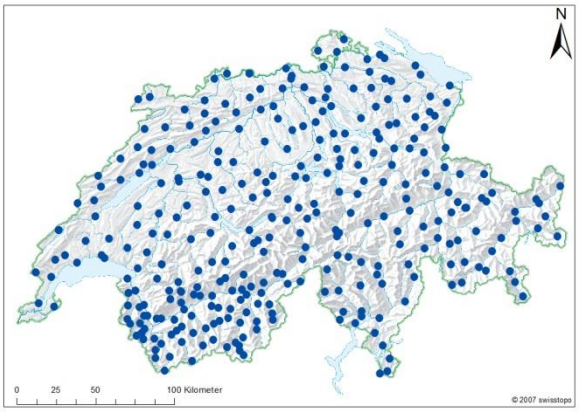

Figure 10 *Final state of the SwissMetNet ground-based meteorological network.*

Developments on data transfer from the meteorological station to the central server using satellite as redundancy to the standard GPRS technology has been successfully tested and implemented.

4.2 WMO CIMO SPICE

SPICE (Solid Precipitation Intercomparison Experiment) is a WMO/CIMO multi-sites intercomparison of instruments and systems of observation for the measurement of solid precipitation. One of the main objectives is the assessment of a wide range of instruments under various climates. For that purpose, around 20 sites worldwide are equipped and configured according to standards defined within the project, in order to allow comparison between the sites. The field experiment started in October 2013 and has been terminated in Summer 2015, so that each site could collect data during two winter seasons.

At an elevation of 2500 m above sea level, the Weissfluhjoch (Davos, Switzerland) contains a SPICE site that has been set up by MeteoSwiss in close collaboration with the Swiss Institute for Snow and Avalanche Research (SLF), owner of the site, to provide reference measurements for the alpine climate (Figure 11 and Figure 12). Among others, a reference set of instruments consisting of three Ott Pluvio^2 weighting gauges – one in a DFIR (Double Fence Intercomparison Reference), one with an Alter shield and one unshielded – will provide data sets for reference measurements analysis. A strong focus will be given to develop a methodology for precipitation phase discrimination using an optical disdrometer, and to link solid precipitation measurements with snow on the ground measurements using various manual and automatic methods.

Figure 11 The SPICE reference site at Weissfluhjoch (Davos).

Figure 12 The reference measurement : the DFIR with an OTT Pluvio^2 weighting gauge on his center and a disdrometer. Other instruments for temperature, humidity, wind give ancillary data around the gauge measurement.

Additional instruments under tests (provided by the manufacturers) are also installed, as for example precipitation gauges, precipitation laser monitor, GPS for snow on the ground, etc. Ancillary measurements (wind, temperature, pressure, humidity, solar radiation) are provided both from the SLF test site and from MeteoSwiss installations. A high resolution camera takes pictures of the gauges orifice. All collected data have been transferred to the SPICE data base, being then available for data analysis, together with the other reference sites.

MeteoSwiss, as weather services of an alpine country, has a great interest in SPICE and its possible outcome. A strong effort (financial, HR) has been, and will be, put on this project (eg. construction of the DFIR, internship). During the whole project, MeteoSwiss has engaged two interns during one year, one of whom staying for the entire project and being financed by Environment Canada and MeteoSwiss (under a MeteoSwiss contract in 2014-15, and as a consultant within WMO in 2016).

The SPICE final report, containing analysis of all sensors under test against the reference, as well as recommendations for the operation of various measurement systems as a whole (instrument, shield, heating, etc.), will be presented during the CIMO/TECO 2016 (27-30 September 2016, Madrid).

Main activities that TB/LC carried out in the last 2 years for which results will soon be available:

- Raman lidar measurements of tropospheric temperature: validation in progress.
- Ceilometer calibration and retrieval of optical aerosol parameters from Raman lidar.
- Automatic detection of the PBL using ground-based remote sensing systems: publication in preparation.
- Performance evaluation of the radiometers designed for the solar energy sector: report in

preparation.

- SPICE experiment (final report + publications to be written).

Which guidance documents/standard procedures were developed during the last 2 years (please include full reference and web-link if available)?

-

Which IOM reports / peer-reviewed publications were published in the last 2 years (please include full reference and web-link if available)?

- Cirisan, A., Luo, B. P., Engel, I., Wienhold, F. G., Sprenger, M., Krieger, U. K., Weers, U., Romanens, G., Levrat, G., Jeannet, P., Ruffieux, D., Philipona, R., Calpini, B., Spichtinger, P., and Peter, T.: Balloon-borne match measurements of midlatitude cirrus clouds, Atmos. Chem. Phys., 14, 7341-7365, doi:10.5194/acp-14-7341-2014, 2014. http://www.atmos-chem-phys.net/14/7341/2014/
- Collaud Coen, M., Praz, C., Haefele, A., Ruffieux, D., Kaufmann, P., and Calpini, B.: Determination and climatology of the planetary boundary layer height above the Swiss plateau by in situ and remote sensing measurements as well as by the COSMO-2 model, Atmos. Chem. Phys., 14, 13205-13221, doi:10.5194/acp-14-13205-2014, 2014. http://www.atmos-chem-phys.net/14/13205/2014/
- Haefele A and D. Ruffieux: Validation of the 1290 MHz wind profiler at Payerne, Switzerland, using radiosonde GPS wind measurements. Meteorol. Appl 22, 873-878, 2015. http://onlinelibrary.wiley.com/doi/10.1002/met.1507/full
- Illingworth A.J., D. Cimini, C. Gaffard, M. Haeffelin, V. Lehmann, U. Löhnert, E. J. O'Connor, and D. Ruffieux, 2015: Exploiting Existing Ground-Based Remote Sensing Networks to Improve High-Resolution Weather Forecasts. *Bull. Amer. Meteor. Soc.*, **96**, 2107–2125. http://dx.doi.org/10.1175/BAMS-D-13-00283.1

- Kräuchi, A., Philipona, R., Romanens, G., Hurst, D. F., Hall, E. G., and Jordan, A. F.: Controlled weather balloon ascents and descents for atmospheric research and climate monitoring, Atmos. Meas. Tech. Discuss., 8, 12559-12588, doi:10.5194/amtd-8-12559-2015, 2015. http://www.atmos-meas-tech-discuss.net/amt-2015-266/

- Kräuchi A. and Rolf Philipona: Return glider radiosonde for in-situ upper-air research measurements . Atmos. Meas. Tech.,Discuss., doi:10.5194/amt-2016-35. http://www.atmos-meas-tech-discuss.net/amt-2016-35/

- Sica R.J. and A. Haefele, Retrieval of temperature from a multiplechannel Rayleigh-scatter lidar using an optimal estimation method. Appl. Opt. 54, 1872–1889 (2015). https://www.osapublishing.org/ao/abstract.cfm?uri=ao-54-8-1872

- Sica R.J. and A. Haefele, Retrieval of water vapor mixing ratio from a multiple channel Raman-scatter lidar using an optimal estimation method, Appl. Opt. 55, 763-777 (2016). https://www.osapublishing.org/ao/abstract.cfm?uri=ao-55-4-763

- Badosa, J., J. Wood, P. Blanc, C. N. Long, L. Vuilleumier, D. Demengel, and M. Haeffelin (2014). Solar irradiances measured using SPN1 radiometers: uncertainties and clues for development, , Atmospheric Measurement Techniques, **7**, 4267-4283, doi:10.5194/amt-7-4267-2014. http://www.atmos-meas-tech.net/7/4267/2014/amt-7-4267-2014.html

- Vignola, F.; Derocher, Z.; Peterson, J.; Vuilleumier, L.; Félix, C.; Gröbner, J., and Kouremeti, N. (2016). Effects of changing spectral radiation distribution on the performance

of photodiode pyranometers. Solar Energy, **129**, 224-235, doi: 10.1016/j.solener.2016.01.047. http://scholar.google.ch/scholar?q=Solar+Energy,+129,+224-235&hl=fr&as_sdt=0&as_vis=1&oi=scholart&sa=X&ved=0ahUKEwiQktnv1rPLAhXHlSwKHWieBRMQgQMIGzAA

- Vuilleumier, L., M. Hauser, C. Félix, F. Vignola, P. Blanc, A. Kazantzidis, and B. Calpini (2014). Accuracy of ground surface broadband shortwave radiation monitoring, J. Geophys. Res. Atmos., **119**:D24, 13'838-13'860, doi:10.1002/2014JD022335. http://onlinelibrary.wiley.com/doi/10.1002/2014JD022335/full

Title(s) of IOM report(s) presently being developed by your Testbed/Lead Centre: (please specify level of development: draft, ready for review, …)

-

Has your Testbed/Lead Centre collaborated with one or more CIMO Expert Teams in developing guidance material? Yes/No Yes

If yes, with which CIMO Expert Team(s)?

Strong relations were maintained with the Lindenberg DWD site for various GRUAN activities as well as with Table Mountain (USA) for Raman lidar activities.

Strong relations with the Expert Team on Instrument Inter-comparisons and with Expert Team on Operational In Situ Technologies.

Capacity Building and Training Activities

Which capacity building/training activities have been carried out by the Testbed in the last 2 years?

- A regular teaching activity (about once a year) is performed with staff from the Kenyan Meteorological Service (KMD) at Nairobi (radiosounding and Dobson)

Has your testbed developed a twinning activity / special relationship with a companion station/site from a developing country? Yes/No Yes

If yes, with which station/site?

A continuous collaboration is maintained between Meteoswiss and the Kenyan Meteorological Service (KMD) at Nairobi. The main focus of this partnership is the ozone measurements with both in-situ (radiosounding) and remote sensing (Dobson) ozone measurements

Is your Testbed/Lead Centre making an oral/poster presentation at this year's TECO? Yes / No
(If yes, please specify Title(s) and Author(s) of the presentation(s)) YES

- A special session on Inter-comparisons including SPICE results will be organized during the coming TECO

Recent Changes in Circumstance

Have there been any recent changes in your Test Bed/Lead Centre's capabilities? If so, please specify:

-

Have there been any recent changes in your Test Bed/Lead Centre's infrastructure? If so, please specify:

-

Have there been any recent changes in your staffing? If so, please specify, and advise whether replacement staff have the required competencies:

-

Future Plans

What are your plans for the next two years?

- Continuation of the efforts to develop Payerne as a GRUAN site (renewal of the radiosonde).
- Reinforcement of the lidar–related activities (both Raman lidar and ceilometers).
- Finalization of the SPICE experiment.

Is your Testbed/Lead Centre able to continue in the role of a Test Bed/Lead Centre during the coming two years?	Yes / No YES

Other relevant information (other activities of special interest to CIMO, etc…)

-

11 March, 2016 — **Date**

Dominique Ruffieux — **Name of Person Filling the Form**